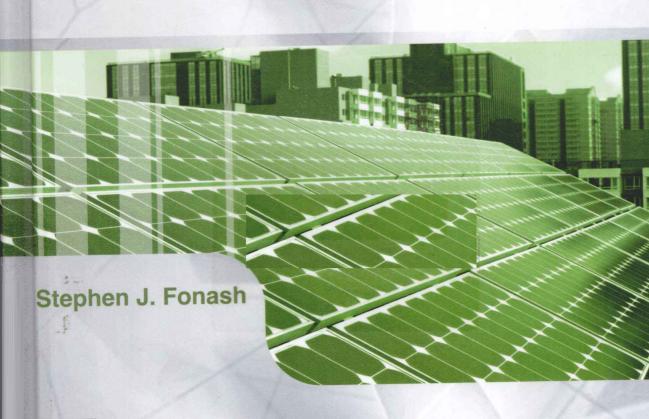


新能源技术应用系列

# 太阳电池器件物理

(原著第2版)

Solar Cell Device Physics (Second Edition)







#### 图字:01-2011-3197号

This is a annotated version of **Solar Cell Device Physics** (**Second Edition**) by Stephen J. Fonash

Copyright 2010, Elsevier Inc. ISBN: 9780123747747

Authorized English language reprint edition published by the Propretor.

Printed in China by Science Press under special arrangment with Elsevier (Singapore) Pte Ltd. This edition if authorized for sale in China only, excluding Hong Kong SAR, Maao SAR and Taiwan. Unauthorized export of this edition is a violoation of the Copyrigt Act. Violation of this Law is subject to Civil and Criminal Penalties.

本书英文影印版由 Elsevier(Singapore)Pte Ltd. 授权科学出版社在中国大陆境内独家发行。本版权在中国境内(不包括香港特别行政区以及台湾)出版及标价销售。未经许可之出口,视为违反著作权法,将受法律之制裁。

### 图书在版编目(CIP)数据

太阳电池器件物理=Solar Cell Device Physics, 英文/(美)福纳什(Fonash, S.)编著.—2版.—北京,科学出版社,2011

ISBN 978-7-03-031237-2

I. ①太… II. ①福… III. ①太阳能电池-元器件-英文 Ⅳ. ①TM914. 4 中国版本图书馆 CIP 数据核字(2011)第 100934 号

> 责任编辑:霍志国/责任印制:钱玉芬 封面设计:耕者设计工作室

#### **希学会展** 社 出版

北京东黄城根北街 16 号 邮政编码:100717

http://www.sciencep.com

## 北京住信远欣艺术印刷有限公司 印刷

科学出版社发行 各地新华书店经销

2011年6月第 一 版

开本:B5(720×1000)

2011 年 6 月第一次印刷

印张:24 1/2 字数:491 000

印数:1-1 800

00 00 =

定价:108.00元 (如有印装质量问题,我社负责调换)

## 导 读

人类的生存离不开能源,地球上能源消耗的主体是不可再生的化石燃料,由此引发的能源危机和环境恶化已成为人类亟待解决的首要问题。太阳能作为一种可再生能源,具有资源丰富、无污染、应用不受地理条件限制等特点,是未来能源结构的基础。太阳能光伏技术是太阳能利用的重要领域之一,而作为太阳能发电的基本装置——太阳电池也成为各国科学家的研究焦点。

1954年,世界上第一块单晶硅太阳电池在贝尔实验室诞生,经过几十年的发展,硅太阳电池的功率转换效率已经超过 25%,但是高昂的成本和复杂的制作工艺限制了其民用化应用。为此,人们积极发展基于半导体薄膜技术的太阳电池。这类太阳电池由于在衬底上沉积很薄的光电材料,大大减小了半导体材料的消耗,降低了制作成本。薄膜太阳电池的材料主要为砷化镓、碲化镉、铜铟镓硒等化合物半导体,存在毒性及资源限制等问题,限制了其大规模实用化发展。

除无机半导体材料外,人们也尝试使用有机半导体作为太阳电池的核心材料。有机太阳电池材料主要是一些具有较大共轭结构的有机小分子、聚合物或金属配合物等,其优势在于有机化合物易于分子剪裁、成本低、器件制备工艺简单并可在卷曲折叠的衬底上制成柔性薄膜电池,受到广泛关注。得益于持续的技术发展和材料创新,目前有机薄膜太阳电池已达到约8%的功率转换效率。然而,受电池结构影响,其光捕获、激子解离效率较低,光谱吸收范围窄。因此,在未来发展还需通过增加光吸收、提高激子解离和载流子收集来改善器件性能。

随着纳米技术的发展,基于纳米结构材料的激子太阳电池成为太阳光伏技术领域的研究热点之一。自从 1991 年 Gratzel 小组报道了染料敏化二氧化钛纳米晶薄膜太阳电池的突破性工作以来,全世界范围内掀起了对染料敏化太阳电池的研究热潮。该种电池的核心包括染料敏化的二氧化钛纳米晶光阳极、纳米铂沉积的对电极以及空穴输运材料,其基本工作原理是染料分子吸收光子从基态跃迁到激发态,激发态的染料分子将电子注入到二氧化钛导带中;而停留在染料分子上的空穴转移到空穴输运材料上,并输运到对电极;二氧化钛中的电子扩散到集流器,经外电路做功后到达对电极,与空穴复合,完成一次循环。经过近 20 年的努力,染料敏化太阳电池的功率转换效率已经达到约 12%,而其成本只有传统硅基电池的 1/5~1/10,显示出广阔的应用前景。

太阳电池进行能量转换的关键步骤包括光捕获、电荷分离以及载流子收集,这些物理过程制约着器件性能,因此对太阳电池能量转换关键步骤的定量描述显

得尤为重要。这不仅可以更加全面系统地理解太阳电池的工作原理,而且对于太阳电池材料的选择与器件结构的优化具有指导意义。本书利用数值分析与解析分析方法对同质结太阳电池、半导体-半导体异质结太阳电池、表面势垒太阳电池以及染料敏化太阳电池进行了深入研究,定量描述了器件中电荷产生、分离与复合过程,及其对器件性能的影响。全书由以下7部分组成:

第1章为本书的引言部分,介绍了太阳电池进行能量转换的4个基本步骤: (1) 吸光材料吸收光子从基态跃迁到激发态,(2) 激发态转化成带正电荷和带负电荷的自由载流子,(3) 根据不同的输运机理,带正电荷的载流子向阳极运动,带负电荷的载流子向阴极移动,(4) 经外电路负载做功后,正电荷与负电荷载流子复合,使吸光材料回到基态。本章也介绍了太阳的光谱分布以及典型太阳电池的器件结构和评价方法。

第2章对太阳电池进行能量转换的基础——材料性质和器件物理进行了阐述。为了构思新的光伏能量转换方案,改进已有的器件结构,开发新型的电池材料,深刻理解光伏器件的材料性质与器件工作条件下的物理基础,需要结合各种特征和现象,如纳米尺度形貌、无定形材料、有机材料、等离子体、量子限域和产生激子的吸收等,并根据各种模型背后的假设条件来更好地判断模型的适用性并做出必要的调整。本着这个思路,作者对太阳电池材料的一些基本性质进行了综述,包括材料的结构、声子谱、能级、光学性质以及载流子的产生、复合与捕获等,并详细讨论了太阳电池中载流子在体相与表面的输运过程,给出了描述稳态条件下太阳电池内部物理机制的数学表达式。

第3章讨论了太阳电池的器件结构、关键材料以及它们的尺寸效应。光伏作用的核心是电荷分离过程,其驱动力可能来自内建电场、有效场或者电子与空穴扩散的差别。作者通过列举3种最基本的能级结构分别对这3种电荷分离驱动力进行了讨论,总结了太阳电池实际工作中的电荷分离驱动力主要来自内建电场或有效场,以及在实际中如何构建太阳电池。本章也对构成太阳电池的吸光材料、辅助材料的性质及要求做了详细的分析与讨论。吸光材料是太阳电池的光捕获剂,其吸收光谱应与太阳光谱匹配,并在受光激发后能产生激子或者自由电子与空穴。除吸光材料外,辅助材料也是太阳电池的重要组成部分。有些辅助材料能够支持一种载流子输运而阻挡另一种载流子通过,确保两种载流子向相反的方向输运,抗反射材料可增加电池的光捕获效率,而导电材料提供了电池电极与外部电路的欧姆接触。这些材料的选择必须保证太阳电池最低的光学和电学上的损失。本章最后讨论了材料与结构的尺寸效应对器件在光学与电学方面的影响。

第 4 章对同质结太阳电池进行了系统全面的阐述。这类太阳电池是建立在对同一种半导体材料进行两种类型掺杂基础上的 p-n 或 p-i-n 结构器件。由于在结附近的内建电场不足以驱动激子解离,因此同质结太阳电池的吸光材料全部是光

激发后直接产生电子与空穴的材料。在 pn 结构器件中,光照产生的少数载流子扩散到 p-n 结区域,这里形成的内建电场通过漂移作用将电子与空穴推向不同的方向来实现电荷分离。而在 p-i-n 结构的器件中,电荷的分离和收集则完全通过漂移来实现。作者首先利用数值分析方法对稳态条件下器件工作的数学表达式求解,分析了空穴输运——电子阻挡和电子输运——空穴阻挡接触材料以及后表面高低掺杂结构对器件的影响,定量描述 p-n 或 p-i-n 同质结太阳电池在暗处和光照条件下的内建电场、复合及电流。随后讨论了利用解析分析方法对 p-n 同质结在光下和偏压下的特性进行了描述,根据方程表达式来研究同质结器件的电流电压特性的起源。

第5章对半导体-半导体异质结太阳电池进行了系统的分析。与同质结太阳电池不同,这类器件使用两种不同的半导体材料,其中一种为吸光材料,另一种可以是吸光材料或者是不吸光的窗口材料。因此出现了一些新的问题,如两种半导体材料的化学相容性和稳定性,化学和物理界面的再现性,而对于晶体和多晶材料还存在晶格的匹配性等,并由此引入了一个新的电荷损失机制,即异质结界面复合。但是异质结也有其固有的优点,例如可以选择某些只能 n 掺杂或只能 p 掺杂的半导体材料,两种半导体材料电子亲和势的差别可以驱动激子解离成自由电子与空穴等。本章首先在输运和势垒区两个方面比较了异质结太阳电池与同质结太阳电池的共同点以及区别。利用数值分析方法对太阳电池的非线性方程求解,分别对光激发产生自由电子与空穴、光激发产生激子这两种情况进行了讨论。随后讨论了解析分析方法及一些假设和边界条件,使用方程表达式对异质结器件的电流电压特性的起源进行了描述。

第6章论述了表面势垒太阳电池。这类太阳电池基于单一掺杂类型的一种半导体材料,其电荷分离的驱动力来自半导体表面的静电场势垒,这种表面势垒宽度可能贯穿整个半导体材料,类似于 p-i-n 结构的情况,也可能只局限在半导体表面附近。表面势垒太阳电池分为两种类型,一种利用金属与半导体电化学势的不同,在半导体一侧建立表面静电场,通常被称作肖特基势垒太阳电池,另一种利用电解质与半导体电化学势的不同建立表面静电场,通常被称作电化学光伏电池。作者回顾了表面势垒太阳电池的发展历史以及现状,概述了器件中的输运及复合过程,以及激子或自由电荷在势垒区的分离过程。作者利用数值分析方法对太阳电池的数学模型进行数值求解,讨论了表面势垒太阳电池电流电压特性的影响因素。随后又利用解析分析方法从载流子产生与复合方面对器件的电流电压关系进行了表达式描述。作者也提到了某些基于纳米结构的表面势垒器件。

第7章介绍了染料敏化太阳电池这种新型光伏器件结构。介绍了器件的工作原理,从连续方程出发,讨论了这种器件的载流子输运及复合过程。染料敏化太阳电池是典型的激子太阳电池,与只利用内建静电场实现电荷分离的 p-n 同质结

太阳电池不同,染料敏化太阳电池中没有内建电场,激子只能通过染料与半导体之间的能级差形成的有效场解离成自由电子与空穴,这点类似于光吸收产生激子的异质结器件。对于这种器件,作者利用数值分析方法对第2章给出太阳电池工作原理的数学表达式求解,定量讨论了器件工作条件下,激子解离、电荷输运与复合过程对器件电流电压输出的影响。此外,作者也讨论了基于固态空穴输运材料的染料敏化太阳电池的器件结构。

王 鹏

中国科学院长春应用化学研究所

正如第 1 版《太阳电池器件物理》一样,本书的重点依然是光伏器件的材料、结构和器件物理。自第 1 版出版以来,光伏领域发生了很大变化,例如出现了激子太阳电池和纳米技术。抓住这些进展的本质对于写作来说是非常有趣的事情,同时也是一种挑战。最终的结果是,新版的《太阳电池器件物理》几乎完全重写了。在新版中,我们对所有光伏领域的发展使用了统一的方法。例如,这个统一的方法要求所有太阳电池,无论其是吸收光子产生激子还是直接产生自由电子空穴对,都需要满足相同的条件,即需要太阳电池具有一种可以打破自由电子与空穴的对称性的结构。打破电子与空穴的对称性是确保太阳电池产生电能的必要条件。本书的观点是:内建静电场或由于态密度分布的空间变化(能级位置、数目或者两者的变化)所引起的内建有效场是打破电子与空穴对称性的原因。例如,内建电场的方法常常应用于经典的硅 p-n 结太阳电池,而有效场则适用于染料敏化太阳电池。

本书利用解析分析和数值分析方法对太阳电池结构进行分析来理解和探索器件物理。解析分析方法的大部分细节被列在附录中,以便读者的思路不会被复杂的方程推导所打断。数值分析方法采用的是作者研究组大量使用的微电子和光伏结构分析软件(AMPS)。本书在引言部分介绍了 AMPS 以便更好地理解光伏作用的起源。在随后的各章节中,AMPS 被用来细致研究各种具体电池类型,如无机 p-n 结太阳电池、有机异质结太阳电池和染料敏化太阳电池。计算机建模给出了电池暗处和光下的电流电压特性,更重要的是,它可用来"撬开太阳电池"以便细致考查工作条件下电池的电流组分、电场和复合。书中讨论的各种例子可以在 AMPS 网站上获得(www. ampsmodeling. org)。本书的宗旨是希望读者能够更详细地研究数值模拟事例,或者将它们作为工具来进一步探索器件物理。

应当指出的是,某些作者特别的处理事情的方式已经渗透到本书中。例如,许多教科书使用 q 作为电子的电量,但是在本书中通篇使用了符号 e 来代表电量。还有随机热能计量 kT,在文中以电子伏特为单位(室温下为 0.026eV)。这意味着在别处被写作  $e^{qV/kT}$  的公式在本书中写作  $e^{V/kT}$ ,其中 V 的单位为伏特,kT 的单位是电子伏特。这也意味着像爱因斯坦关系式这种用来描述空穴扩散系数  $D_p$  和迁移率  $\mu_p$  关系的表达式,在本书中写作  $D_p = k$  T  $\mu_p$  。

光伏电池作为替代能源将持续快速发展,并越来越显示出它的重要性。虽然

在相关的器件章节里简要概括了光伏电池的历史以及发展现状,但是本书的主旨 并不是对其进行一个全面的回顾,而是为了让读者从本书中了解太阳电池的基本 原理,跟上这一令人兴奋的领域的发展步伐,并为其成长做出贡献。

(王 鹏 译)

# **Preface**

As was the case with the first edition of Solar Cell Device Physics, this book is focused on the materials, structures, and device physics of photovoltaic devices. Since the first edition was published, much has happened in photovoltaics, such as the advent of excitonic cells and nanotechnology. Capturing the essence of these advances made writing both fun and a challenge. The net result is that Solar Cell Device Physics has been almost entirely rewritten. A unifying approach to all the developments is used throughout the new edition. For example, this unifying approach stresses that all solar cells, whether based on absorption that produces excitons or on absorption that directly produces free electron-hole pairs, share the common requirement of needing a structure that breaks symmetry for the free electrons and holes. The breaking of symmetry is ultimately what is required to enable a solar cell to produce electric power. The book takes the perspective that this breaking of symmetry can occur due to built-in electrostatic fields or due to built-in effective fields arising from spatial changes in the density of states distribution (changes in energy level positions, number, or both). The electrostatic-field approach is, of course, what is used in the classic silicon p-n junction solar cell. The effective-fields approach is, for example, what is exploited in the dye-sensitized solar cell.

This edition employs both analytical and numerical analyses of solar cell structures for understanding and exploring device physics. Many of the details of the analytical analyses are contained in the appendices, so that the development of ideas is not interrupted by the development of equations. The numerical analyses employ the computer code Analysis of Microelectronic and Photovoltaic Structures (AMPS), which came out of, and is heavily used by, the author's research group. AMPS is utilized in the introductory sections to augment the understanding of the origins of photovoltaic action. It is used in the chapters dedicated to different cell types to give a detailed examination of the full gamut of solar cell types, from inorganic p—n junctions to organic heterojunctions

and dye-sensitized cells. The computer modeling provides the dark and light current voltage characteristics of cells but, more importantly, it is used to "pry open cells" to examine in detail the current components, the electric fields, and the recombination present during operation. The various examples discussed in the book are available on the AMPS Web site (www.ampsmodeling.org). The hope is that the reader will want to examine the numerical modeling cases in more detail and perhaps use them as a tool to further explore device physics.

It should be noted that some of the author's specific ways of doing things have crept into the book. For example, many texts use q for the magnitude of the charge on an electron, but here the symbol e is used throughout for this quantity. Also kT, the measure of random thermal energy, is in electron volts (0.026 eV at room temperature) everywhere. This means that terms that may be written elsewhere as  $e^{qV/kT}$  appear here as  $e^{V/kT}$  with V in volts and kT in electron volts. It also means that expressions like the Einstein relation between diffusivity  $D_p$  and mobility  $\mu_p$  for holes, for example, appear in this book as  $D_p = kT\mu_p$ .

Photovoltaics will continue to develop rapidly as alternative energy sources continue to gain in importance. This book is not designed to be a full review of where we have been or of where that development is now, although each is briefly mentioned in the device chapters. The intent of the book is to give the reader the fundamentals needed to keep up with, and contribute to, the growth of this exciting field.

# Acknowledgments

As with the first edition, this book has grown out of the graduate-level solar cell course that the author teaches at Penn State. It has profited considerably from the comments of the many students who have taken this course. All the students and post-docs who have worked in our research group have also contributed to varying degrees. Outstanding among these is Dr. Joseph Cuiffi who aided greatly in the numerical modeling used in this text.

The efforts of Lisa Daub, Darlene Fink and Kristen Robinson are also gratefully acknowledged. They provided outstanding assistance with figures and references. Dr. Travis Benanti, Dr. Wook Jun Nam, Amy Brunner, and Zac Gray contributed significantly in various ways, from proofreading to figure generation. The help of all these people, and others, made this book a possibility. The encouragement and understanding of my wife Joyce made it a reality.

# **List of Symbols**

Element	Description (Units)
α	Absorption coefficient (nm <sup>-1</sup> , cm <sup>-1</sup> )
$\beta_1$	Dimensionless quantity describing ratio of n-portion quasi-neutral region length to hole diffusion length
$\beta_2$	Dimensionless quantity describing ratio of n-portion quasi-neutral region length to the absorption length
$\beta_3$	Dimensionless quantity describing ratio of top-surface hole carrier recombination velocity to hole diffusion- recombination velocity in the n-portion
$\beta_4$	Dimensionless quantity describing ratio of the absorber thickness up to the beginning of the quasi-neutral region in the p-portion to absorption length
$\beta_5$	Dimensionless quantity describing ratio of p-portion quasi-neutral-region length to electron diffusion length
$\beta_6$	Dimensionless quantity describing ratio of the p-portion quasi-neutral-region length to absorption length
$\beta_7$	Dimensionless quantity describing ratio of back-surface electron carrier recombination velocity to the electron diffusion-recombination velocity
γ	Band-to-band recombination strength parameter $(cm^3s^{-1})$
Δ	Magnitude of the energy shift caused by an interface dipole (eV)
Δ	Thickness of dye monolayer in DSSC (nm)
Δ	Grain size in polycrystalline materials (nm)
$\Delta_{ m C}$	Conduction-band offset between two materials at a heterojunction (eV)

$\Delta_{ m V}$	Valence-band offset between two materials at a heterojunction (eV)
$\Phi_0(\lambda)$	Photon flux per bandwidth as a function of wavelength $(m^{-2}s^{-1}$ per bandwidth in nm)
$\phi_{\mathbf{B}}$	Schottky barrier height of an M-S or M-I-S structure (eV)
$\varphi_{\mathbf{B}\mathbf{I}}$	Energy difference between $E_C$ and $E_F$ for an n-type material or the energy difference between $E_F$ and $E_V$ for a p-type material at the semiconductor surface in an M-I-S structure (eV)
$\Phi_{ m C}$	Photon flux corrected for reflection and absorption before entering a material ( $cm^{-2}s^{-1}$ per bandwidth in nm)
$\varphi_{\boldsymbol{W}}$	Workfunction of a material (eV)
$\varphi_{\textbf{WM}}$	Workfunction of a metal (eV)
$\varphi_{\mathbf{W}n}$	Workfunction of an n-type semiconductor (eV)
$\varphi_{Wp}$	Workfunction of a p-type semiconductor (eV)
ε	Permittivity (F/cm)
η	Device power conversion efficiency
λ	Wavelength of a photon or phonon (nm)
$\mu_{Gi}$	Mobility of charge carriers in localized gap states $(cm^2/V-s)$
$\mu_n$	Electron mobility (cm <sup>2</sup> /V-s)
$\mu_{p}$	Hole mobility (cm <sup>2</sup> /V-s)
ν	Frequency of electromagnetic radiation (Hertz)
ξ	Electric field strength (V/cm)
$\xi_0$	Electric field present at thermodynamic equilibrium (V/cm)
$\xi'_n$	Electron effective force field (V/cm)
ξ' <sub>p</sub>	Hole effective force field (V/cm)
ρ	Charge density (C/cm <sup>3</sup> )

$\sigma_n$	Cross-section of a localized state for capturing an electron $(\mbox{cm}^2)$
$\sigma_{\mathbf{p}}$	Cross-section of a localized state for capturing a hole $(cm^2)$
$ au_{\mathbf{E}}$	Exciton lifetime (s)
$ au_{ m n}$	Electron lifetime (dictated by $\tau_n^R$ , $\tau_n^L$ , or $\tau_n^A$ ) for p-type material (s)
$ au_n^A$	Electron Auger lifetime for p-type material (s)
$ au_{ m n}^{ m L}$	Electron S-R-H recombination lifetime for p-type material $(s)$
$\tau_n^R$	Electron radiative recombination lifetime for p-type material (s)
$ au_{ m p}$	Hole lifetime (dictated by $\tau_p^R$ , $\tau_p^L$ , or $\tau_p^A$ ) for n-type material (s)
$ au_{ m p}^{ m A}$	Hole Auger lifetime for n-type material (s)
$ au_p^A \  au_p^L$	Hole S-R-H recombination lifetime for n-type material (s)
$ au_p^R$	Hole radiative recombination lifetime for n-type material (s)
χ	Electron affinity (eV)
a	Lattice constant (nm)
$A_{abs}$	Absorbance
<b>A*</b>	Effective Richardson constant $(120  \text{A/cm}^2/\text{K}^2  \text{for free})$ electrons) $(\text{A/cm}^2/\text{K}^2)$
$A_{1A}^A$	Rate constant for the Auger recombination shown in Figure 2.18a (cm <sup>6</sup> /s)
$A_{1B}^A$	Rate constant for the Auger recombination shown in Figure 2.18b (cm <sup>6</sup> /s)
$A_{1C}^{A}$	Rate constant for the Auger transition shown in Figure 2.18c (cm <sup>6</sup> /s)
$A_{1D}^A$	Rate constant for the Auger transition shown in Figure 2.18d (cm <sup>6</sup> /s)

$A_{1E}^{A}$	Rate constant for the Auger transition shown in Figure 2.18e (cm <sup>6</sup> /s)
$A_{1F}^A$	Rate constant for the Auger transition shown in Figure 2.18f (cm $^6$ /s)
A <sub>2A</sub>	Rate constant for the Auger generation corresponding to Figure 2.18a (s $^{-1}$ )
$A_{2B}^A$	Rate constant for the Auger generation corresponding to Figure 2.18b (s $^{-1}$ )
$A_{\rm C}$	Solar cell area collecting photons in a concentrator cell $(cm^2 \ or \ m^2)$
$A_{\rm C}$	Used in the density of states model $g_e^c(E) = A_c(E - E_c)^{1/2} (cm^{-3} eV^{3/2})$
$A_S$	Solar cell area generating current in a concentrator cell $(cm^2 \text{ or } m^2)$
$A_{V}$	Used in the density of states model $g_e^v(E) = A_v(E_v - E)^{1/2}(cm^{-3}eV^{3/2})$
c	Speed of light (2.998 $\times$ 10 <sup>17</sup> nm/s)
d	Distance or position in a device (cm, nm)
$D_{E}$	Exciton diffusion coefficient (cm <sup>2</sup> /s)
$D_n$	Electron diffusion coefficient or diffusivity (cm²/s)
$D_n^T$	Electron thermal diffusion (Soret) coefficient (cm <sup>2</sup> /K-s)
$D_p$	Hole diffusion coefficient or diffusivity (cm <sup>2</sup> /s)
$D_p^T$	Hole thermal diffusion (Soret) coefficient (cm <sup>2</sup> /K-s)
e	Charge on an electron $(1.6 \times 10^{-19}  \text{C})$
E	Energy of an electron, photon, or phonon (eV)
$E_C$	Energy of the conduction-band edge, often called the LUMO for organic semiconductors (eV)
$E_{Fn}$	Spatially varying electron quasi-Fermi level (eV)
$E_{Fp}$	Spatially varying hole quasi-Fermi level (eV)
$E_{gm}$	Mobility band gap (eV)

$E_G$	Band gap (eV)
$E_{pn}$	Energy of a phonon (eV)
$E_{pt}$	Energy of a photon (eV)
$E_0$	Energy parameter in the model for the Franz-Keldysh effect defined by $E_0=\frac{3}{2}(m^*)^{-1/3}(e\hbar\zeta)^{2/3}\times 6.25\times 10^{18}$ with $m^*,\hbar,$ and $\zeta$ expressed in MKS units (eV)
$E_{\mathbf{V}}$	Energy of the valence-band edge, often called the HOMO for organic semiconductors (eV)
$E_{VL}$	Vacuum level energy (eV)
F <sub>e</sub>	Total force experienced by an electron where $F_e=-e(\xi-(d\chi/dx)-kT_n(d\ln N_C/dx))$ [Computed using all terms in MKS units. Arises from the electric field and the electron effective field.] (Newtons)
$\mathbf{F}_{\mathtt{h}}$	Total force experienced by a hole where $F_h = e(\xi - (d(\chi + E)/dx) + kT_p(d\ln N_V/dx))$ [Computed using all terms in MKS units. Arises from the electric field and the hole effective field.] (Newtons)
g <sub>A</sub>	Carrier thermal generation rate for Auger process of Figure 2.18a (cm $^{-3}$ -s $^{-1}$ )
A g <sub>B</sub>	Carrier thermal generation rate for Auger process of Figure 2.18b (cm $^{-3}$ -s $^{-1}$ )
g(E)	Density of states in energy per volume (eV <sup>-1</sup> cm <sup>-3</sup> )
g <sub>e</sub> <sup>c</sup> (E)	Conduction-band density of states per volume $(eV^{-1}cm^{-3})$
$g_e^v(E)$	Valence-band density of states per volume ( $eV^{-1}cm^{-3}$ )
$g_{pn}(E)$	Phonon density of states ( $eV^{-1}cm^{-3}$ )
R gth	Number thermally generated electrons in the conduction band and holes in the valence band per time per volume due to band-to-band transitions (cm <sup>-3</sup> -s <sup>-1</sup> )
$G(\lambda, x)$	Number of Processes 3–5 (see Fig. 2.11) absorption events occurring per time per volume of material per bandwidth ( $cm^{-3}$ - $s^{-1}$ - $nm^{-1}$ )

## xx List of Symbols

G'	Exciton generation rate (cm <sup>-3</sup> -s <sup>-1</sup> )
$G_{n}^{"}$	Represents any electron generation rate (cm <sup>-3</sup> -s <sup>-1</sup> )
$G_p$ "	Represents any hole generation rate (cm <sup>-3</sup> -s <sup>-1</sup> )
$G_{ph}^{n}(\lambda,x)$	Free electron generation rate per time per volume of material per bandwidth (cm <sup>-3</sup> -s <sup>-1</sup> -nm <sup>-1</sup> )
$G_{ph}^{p}(\lambda, x)$	Free hole generation rate per time per volume of material per bandwidth (cm <sup>-3</sup> -s <sup>-1</sup> -nm <sup>-1</sup> )
$G_{\text{ph}}(\lambda,x)$	Free carrier generation rate per time per volume of material per bandwidth. [Used when $G^n_{ph}(\lambda,x)=G^p_{ph}(\lambda,x)$ .] $(cm^{-3}\text{-}s^{-1}\text{-}nm^{-1})$
h	Planck's constant $(4.14 \times 10^{-15}  \text{eV-s})$
$\hbar$	Planck's constant divided by $2\pi$ (1.32 $\times$ 10 <sup>-15</sup> eV-s)
$I(\lambda)$	Photon flux impinging on a device (cm <sup>-2</sup> -s <sup>-1</sup> )
I	Electrical current produced by a device (A)
I	Exciton dissociation rate per area of interface $(cm^{-2}-s^{-1})$
I(x)	Intensity (photons per area per bandwidth) of light as it travels through a material (cm <sup>-2</sup> -s <sup>-1</sup> -nm <sup>-1</sup> )
$I_0$	Intensity of incident light (photons per area per bandwidth) (cm <sup>-2</sup> -s <sup>-1</sup> -nm <sup>-1</sup> )
J	Current density; terminal current density emerging from the device (A/cm²)
$J_0$	Pre-exponential term in the multistep tunneling model $J_{MS} = -J_0 e^{BT} e^{AV} (A/cm^2)$
$J_{DK}$	Dark current density (A/cm <sup>2</sup> )
$ m J_{FE}$	Interface current density arising from field emission at a junction (A/cm <sup>2</sup> )
$J_{I}$	Prefactor in the interface recombination current model $\{J_1(e^{V/n_1kT}-1)\}\ (A/cm^2)$